ELSEVIER

Journal of Alloys and Compounds 224 (1995) 168–169

Journal of ALLOYS AND COMPOUNDS

Isothermal section of the phase diagram of the ternary system Nd–Fe–Mn at room temperature

Liu Jingqi

The Industrial Testing and Experimental Centre of Guangxi University, Nanning, Guangxi, People's Republic of China

Received 4 November 1994

Abstract

The isothermal section of the phase diagram of the ternary system Nd–Fe–Mn at room temperature was investigated by X-ray diffraction. The section at room temperature consists of eight single-phase regions, fourteen two-phase regions and seven three-phase regions. The single-phase region τ ($Fe_{20}Mn_{70}Nd_{10}$) in the section is a new ternary intermetallic compound.

Keywords: Isothermal section; Phase diagrams; X-ray powder diffraction

1. Introduction

In Refs. [1,2] the phase diagram of the Fe–Mn system was reported. There exist no intermetallic compounds in this binary system. In Ref. [3] the phase diagram of the Nd–Mn system was reported. There exist two intermetallic compounds in this binary system, but there is some doubt if Mn_2Nd exists. The Fe–Nd binary phase diagram was first reported by V.F. Terekhova et al. [4]. They concluded that there exist two intermetallic compounds, $Fe_{17}Nd_2$ and Fe_2Nd. The existence of Fe_2Nd as a stable phase was also reported in Ref. [5]. However, the existence of Fe_2Nd was not reconfirmed in a later investigation [6].

2. Experimental details

The neodymium, iron and manganese used for the experiments were of 99.9%, 99.99% and 99.9% purity, respectively. The alloy buttons were prepared in an argon atmosphere in a high frequency induction furnace. The melting of all samples was done in alumina crucibles. 150 samples were prepared, each weighing 3 g.

The samples were kept sealed in silica tubes in vacuum during homogenization. The homogenization temperatures of the alloys were chosen on the basis of the binary phase diagrams of the Fe–Mn, Nd–Fe and Nd–Mn systems. The alloys which contained more than 10 at.% Nd were homogenized at 620 °C for 36 days and then cooled at a rate 10 °C h^{-1} to room temperature. The alloys which contained less than 10 at.% Nd were kept at 650 °C–700 °C for 25–30 days and then cooled at a rate 10 °C h^{-1} to room temperature. For alloy powders investigated by X-ray diffraction we used homogenized alloy buttons. The alloy powder was sealed in glass tubes in vacuum. The alloy powders were treated for five days at 500 °C and then cooled at a rate of 10 °C h^{-1} to room temperature.

The X-ray diffraction analysis was performed with powder samples using a Rigaku 3015 diffractometer. A molybdenum target, a voltage of 50 kV, a current of 15 mA and a zirconium filter were used.

3. Result and discussion

3.1. Isothermal section at room temperature

By comparing and analyzing the X-ray diffraction patterns of 150 samples, and by identifying the phases in each sample, the isothermal section of the phase diagram of the ternary system Nd–Fe–Mn was determined at room temperature. It is shown in Fig. 1 that this section consists of eight single-phase regions: α_1(Mn), α_2(Fe), α_3(Nd), γ, β ($Mn_{12}Nd$), φ ($Mn_{23}Nd_6$), δ ($Fe_{17}Nd_2$) and τ ($Fe_{20}Nd_{70}Mn_{10}$); fourteen two-phase regions: $\alpha_1+\gamma$, $\gamma+\alpha_2$, $\alpha_1+\beta$, $\beta+\varphi$, $\alpha_1+\varphi$, $\alpha_1+\tau$, $\tau+\varphi$, $\tau+\gamma$, $\tau+\delta$, $\gamma+\delta$, $\alpha_2+\delta$, $\delta+\alpha_3$, $\delta+\varphi$ and $\varphi+\alpha_3$ and seven three-phase regions: $\alpha_1+\beta+\varphi$, $\alpha_1+\varphi+\tau$, $\varphi+\tau+\delta$, $\tau+\gamma+\delta$, $\tau+\alpha_1+\gamma$, $\gamma+\delta+\alpha_2$ and $\varphi+\alpha_3+\delta$.

3.2. Phase analysis

By analyzing the X-ray diffraction patterns of the Nd–Mn and Nd–Fe system samples we could not

SSDI 0925-8388(95)01544-2

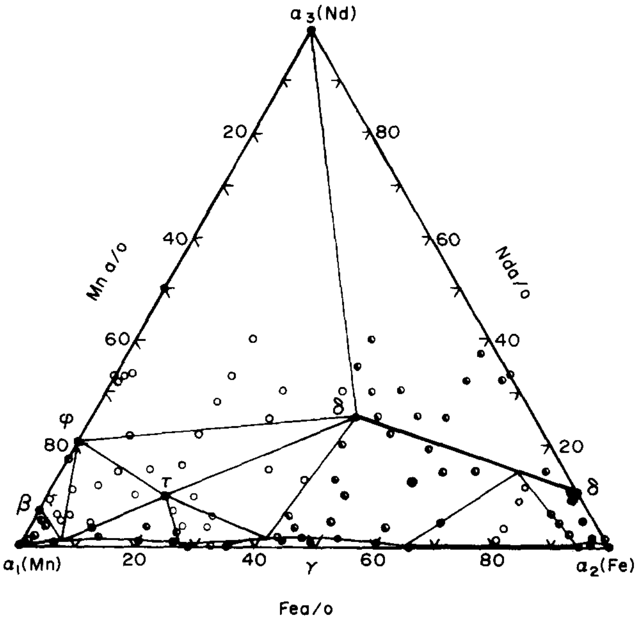

Fig. 1. Isothermal section of the phase diagram of the ternary system Nd–Fe–Mn at room temperature.

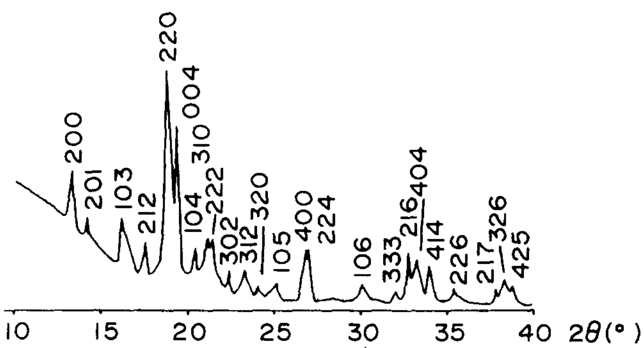

Fig. 2. X-ray diffraction pattern of the τ ($Fe_{20}Mn_{70}Nd_{10}$) phase.

confirm the existence of Mn_2Nd and Fe_2Nd, respectively.

The τ ($Fe_{20}Mn_{70}Nd_{10}$) phase is a new ternary intermetallic compound. The X-ray diffraction pattern of the τ ($Fe_{20}Mn_{70}Nd_{10}$) phase is shown in Fig. 2. The result of the indexing of the new phase τ is shown in Table 1. The tetragonal lattice constants are about $a=(0.61663\pm0.00010)$ nm, $c=(0.84226\pm0.00010)$ nm. The structure and property of the τ phase were not determined. Further work will be carried out.

3.3. Solid solubility

Nd, Fe and Mn can form limited solid solutions at room temperature. The solid solubility of Fe in Mn is about 29 wt.% Fe. The solid solubility of Mn in Fe is about 5 at.% Mn. The Mn and Fe form the intermediate γ phase. The content of Fe in the γ phase is about from 35 at.% Fe to 65 at.% Fe. The solid solubility of the Nd in α_1, α_2 and γ phases is about 1 at.%, 1 at.% and 2 at.% respectively. The γ phase when containing Nd and only Fe or Mn is stable only at high temperatures. However the γ phase, when consisting of 29–95 at.% Fe, 5–71 at.% Mn and 1–2 at.% Nd is still stable at room temperature. The $Fe_{17}Md_2$ phase in the Nd–Fe–Mn ternary system has a range of solid solubility. The formula composition of the $Fe_{17}Nd_2$ phase in the ternary system may be expressed as $Fe_{89.47-(x+y)}Mn_yNd_{10.53+x}$ ($x=0\sim14.47$, $y=0\sim30$) (Fig. 1). The other single-phase fields of solid solution are too small to be observed at room temperature.

Table 1
Powder diffraction date for $Fe_{20}Mn_{70}Nd_{10}$

No	I	hkl	$2\theta_{obs}$ (°)	$2\theta_{cal}$ (°)	$\Delta 2\theta$ (°)
1	63	200	13.30	13.23	−0.07
2	46	201	14.10	14.10	0
3	45	103	16.10	15.99	−0.11
4	37	212	17.52	17.72	0.20
5	100	220	18.80	18.76	−0.04
6	78	004	19.30	19.43	0.13
7	34	104	20.35	20.54	0.19
8	38	310	21.00	21.00	0
9	38	222	21.35	21.15	−0.20
10	24	302	22.35	22.18	−0.17
11	25	312	23.20	23.17	−0.03
12	20	320	24.00	23.98	−0.02
13	21	105	25.10	25.26	0.16
14	33	400	26.70	26.65	−0.05
15	34	224	27.00	27.13	0.13
16	21	106	30.10	30.09	−0.01
17	18	333	31.95	31.96	0.01
18	30	216	32.75	33.00	0.25
19	30	404	33.20	33.20	0
20	28	414	33.90	33.89	−0.01
21	19	226	35.15	35.04	−0.11
22	22	217	37.80	37.59	−0.21
23	22	326	38.30	38.23	−0.07
24	19	425	38.70	38.91	0.21

[a] $2\theta_{obs}$–peak value of diffraction curve.
[b] $\Delta 2\theta = 2\theta_{cal} - 2\theta_{obs}$.

Acknowledgments

This work is supported by the National Science Foundation of China.

References

[1] M. Hansen, *Constitution of Binary Alloys*, McGraw Hill, New York, 2nd edn., 1958, pp. 664–668.
[2] C.J. Smithells, *Metals Reference Book*, Butterworths, London, 5th edn., 1976, p. 605.
[3] H.R. Kirchmayr and W. Luhscheider, *Z. Metallkd., 61* (1970) 22–23.
[4] V.F. Terekhova, E.V. Maslava and Y.M. Savilsky, *Russian Metallurgy (Metally), 3* (1965) 128.
[5] K.A. Gschneidner, *Rare Earth Alloys*, Van Nostrand, New York, 1961.
[6] G. Schneider, E.T. Henig, G. Petzow and H.H. Stadclmaier, *Z. Metallkd., 78* (10) (1987).